Information on Oral Temperature is More Robustly Encoded Than Taste in Neurons of the Mouse Gustatory Cortex

Audrey N. Nash[1], Cecilia G. Bouaichi[2], Katherine E. Odegaard[2], Tom Needham[1], Martin Bauer[1], Richard Bertram[3], and Roberto Vincis[4]

[1]Florida State University, Department of Mathematics
[2]Florida State University, Department of Biological Science and Program in Neuroscience
[3]Florida State University, Department of Mathematics and Programs in Neuroscience and Molecular Biophysics
[4]Florida State University, Department of Biological Science, Programs in Neuroscience, Molecular Biophysics and Cell and Molecular Biology

April 27, 2024

Abbreviated title: Taste and Temperature Encoding in GC Neurons

Corresponding author: Dr. Roberto Vincis, rvincis@fsu.edu

Financial Interests or Conflict of Interest statement: The authors declare no conflict.

Abstract

The gustatory cortex (GC) has traditionally been studied for its role in processing taste stimuli at a fixed temperature. The GC neurons respond to compounds representing different taste qualities and their hedonic value with time-varying and lick-related patterns of activity. However, a growing body of experimental work indicates that GC neurons can also respond to non-gustatory components of oral stimuli, including temperature, a prominent feature of the sensory properties of food and beverages. In this study, our objective is to evaluate the neural saliency of GC neurons in encoding chemosensory taste information at room temperature compared to their responsiveness to oral thermal information, specifically deionized water in the absence of classical taste qualities. To address this question, we recorded spiking activity from over 900 single GC neurons in mice allowed to freely lick to receive four liquid gustatory stimuli at room temperature or deionized water at different non-nociceptive temperatures. We then used a Bayesian analysis approach to determine classification scores for spike trains, considering both the rate and phase codes in response to the different stimuli. Our findings suggest that a classification approach that relies primarily on rate information, with a secondary contribution from phase, is optimal to distinguish between gustatory stimuli or water temperature. Surprisingly, we also observed that the number of GC neurons correctly classifying the stimulus is larger for thermal stimuli than for chemosensory stimuli, indicating that fluid temperature is more strongly encoded and thus more neurally salient than taste information.

Introduction

Eating behaviors are influenced by the initial sensation and the reward experienced when eating food and beverages. This sensation results from the integration of multiple oral signals (Samuelsen and Vincis, 2021; Spence, 2015; Small, 2012; Lemon, 2021). Numerous studies on rodent behavior have described the physiological correlates of one of these sensory components, taste. Using fluid taste stimuli at room temperature, these investigations revealed that taste information undergoes neural computations within interconnected brain regions, including the gustatory cortex (GC), the primary cortical region responsible for processing taste information (Vincis and Fontanini, 2019; Spector and Travers, 2005). GC neurons have shown time-varying patterns of activity in response to chemosensory qualities and the hedonic value of gustatory stimuli, which play

a role in influencing taste-related decisions (Katz et al., 2001; Stapleton et al., 2006; Dikecligil et al., 2020; Jezzini et al., 2013; Levitan et al., 2019). Furthermore, the ability of GC neurons to distinguish between tastes is improved when the rate and timing are interpreted relative to the timing of the licks, indicating that the lick cycle is a key factor in taste processing (Neese et al., 2022).

Several studies indicate that GC neurons also respond to non-gustatory components of oral stimuli (Vincis and Fontanini, 2016; Samuelsen and Fontanini, 2017; Rudenga et al., 2010; Samuelsen and Vincis, 2021), including temperature, a prominent feature of the sensory properties of food and beverages. Studies in humans and primates (Cerf-Ducastel et al., 2001; Verhagen et al., 2004), as well as in anesthetized rats (Yamamoto et al., 1981; Kosar et al., 1986) and investigations by our laboratory in awake mice (Bouaichi et al., 2023), suggest that changes in oral temperature, even in the absence of classical taste qualities, modulate activity in GC neurons. In particular, our recent findings (Bouaichi et al., 2023) revealed that more than half of the GC neurons that encode chemosensory taste stimuli can also discriminate thermal information. Although these data suggest that the GC is a potential key brain region to integrate taste and thermal orosensory input, they do not provide a detailed analysis of its neural responses. Consequently, different aspects of the GC's capability to process taste and oral thermal stimuli are poorly characterized.

The primary objective of this study is to evaluate the neural saliency of GC neurons in encoding chemosensory taste information at room temperature, compared to their ability to integrate oral thermal information. To this end, we collected recordings of spiking activity from more than 900 individual GC neurons in mice allowed to freely lick to receive a small drop (3 μl) of one of four liquid gustatory stimuli (sucrose, NaCl, citric acid and quinine) at room temperature, or deionized water at one of three different non-nociceptive temperatures (14°, 25° and 36°C). Our previous study (Bouaichi et al., 2023) indicated that the responses of GC neurons to different temperatures of deionized water and artificial saliva - a stimulus often used as a neutral control in taste research - were highly similar, supporting the use of deionized water at different temperatures as a thermal stimulus in the absence of overt chemosensory taste information. We then used a Bayesian analysis approach to compute classification scores for spike trains, taking into account both the rate and phase (the timing of spikes within the lick cycle) in response to different oral stimuli. Our results suggest that a classification strategy primarily reliant on rate information, complemented by phase, is optimal for distinguishing between the different gustatory stimuli and

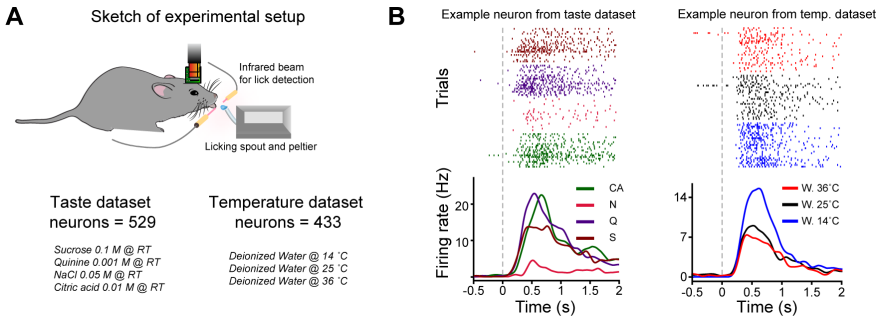

Figure 1: **(A)** Schematic showing the recording setup and a head-restrained mouse licking a spout to obtain oral stimuli. The taste dataset includes GC neurons recorded while animals experience one of four taste stimuli (sucrose 0.1 M, NaCl 0.05 M, citric acid 0.01 M, and quinine 0.001 M) at room temperature. The temperature dataset includes GC neurons recorded while the animals experience deionized water at one of three non-nociceptive temperatures (14°, 25,° 36°C). **(B)** Raster plots and peristimulus time histograms (PSTHs) of 2 representative GC neurons from the taste (left) and temperature (right) dataset.

between the variations in the temperature of deionized water. Furthermore, our analysis revealed that the number of GC neurons that accurately classify oral cues is substantially higher for thermal stimuli than for chemosensory stimuli. This finding suggests that fluid temperature is more robustly encoded, making it more neurally salient compared to the encoding of taste. Finally, analysis of spike trains within individual post-stimulus lick intervals reveals that somatosensory-thermal input is decoded sooner than chemosensory-taste input.

Methods

Experimental design and statistical analysis

Data acquisition

The experiments in this study were conducted on 30 wild-type C57BL/6J adult mice (aged 10–20 weeks; comprising 16 males and 14 females). The mice were acquired from The Jackson Laboratory and upon arrival housed in conditions with a 12/12 hour light/dark cycle, with unrestricted access to food and water. The experiments and training sessions were performed during the light phase of this cycle. All experiments are reviewed and approved by the Florida State University Institutional Animal Care and Use Committee (IACUC) under the

protocol PROTO202100006. A detailed description of surgery, probe implantation, and stimulus delivery can be found in (Bouaichi and Vincis, 2020; Bouaichi et al., 2023; Neese et al., 2022). The voltage signals from the tetrodes were captured, digitized and filtered by bandpass (300-6000 Hz) using the Plexon OmniPlex system at a sampling rate of 40 kHz. For automated spike sorting, Kilosort by Pachitariu et al. (Pachitariu et al., 2016) was used on a workstation equipped with an NVIDIA GPU, CUDA, and MATLAB. After spike sorting, Phy software facilitated manual curation. Subsequently, the quality metrics and waveform characteristics were determined using scripts based on SpikeInterface (Buccino et al., 2020). Only units exhibiting an overall firing rate greater than 0.3 Hz, a signal-to-noise ratio greater than 3.0 and an ISI violation rate less than 0.2 were considered for further analysis. The experimental dataset consists of 962 neurons. The taste dataset (529 neurons) neurons come from a previously published dataset (Neese et al., 2022); neural activity was recorded while the mice were allowed to freely lick to receive 3 μl of one of the four taste stimuli (sucrose, NaCl, citric acid and quinine) at room temperature. The temperature dataset (433 neurons) neurons come from a second previously published dataset (Bouaichi et al., 2023); neural activity was recorded while mice were allowed to freely lick to receive 3 μl of deionized water presented at one of three non-nociceptive temperatures (14°, 25° and 36°C).

At the end of the experiment, the mice were deeply anesthetized for the last time and subjected to transcardial perfusion with 30 ml of PBS, followed by 30 ml of 4% paraformaldehyde (PFA). The brains of the subjects were then removed and further fixed in PFA for 24 hours. After fixation, coronal brain sections (100 µm thick) that included GC were prepared using a vibratome (VT1000 S; Leica, Wetzlar, Germany). To highlight the paths taken by the tetrode bundles and probes, brain sections were counterstained with Hoechst 33342 (1:5000 dilution, H3570; Thermo Fisher, Waltham, MA) using standard techniques and then placed on glass slides. The stained sections of the GC were examined and imaged with a fluorescence microscope.

Data Pre-Processing and Normalization

Raw spike trains are mathematically represented as 4000-dimensional vectors, with one entry (either 0 or 1) per millisecond of experimental data collection. Lick timings are also represented as vectors of the same dimension with entries of either 0 or 1 reflecting the absence or presence of a lick at each time point.

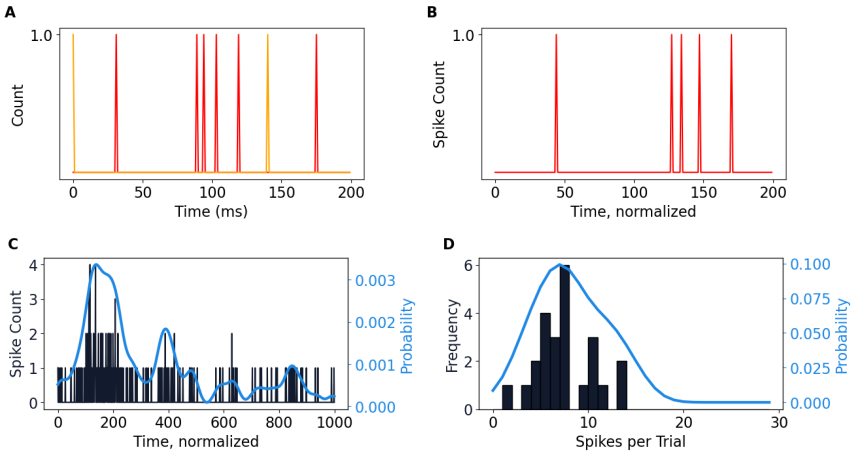

Figure 2: Illustration of the lick interval normalization process and calculation of empirical probability distribution functions. **(A)** A depiction of the timings of the licks (orange) and the neuronal spikes (red). There are 5 spikes within the 140 ms lick interval delimited by the two licks shown. **(B)** The lick interval is extended to 200 ms, preserving the number of spikes and the relative differences in the timing of the spikes. **(C)** For the phase distribution, the black bars indicate the union of all spike times in the processed spike train vectors across all trials. The blue curve is the probability density function generated by kernel density estimation. **(D)** For the rate distribution, the black bars are a histogram showing the frequency of spike numbers per test in a population of processed spike train vectors. The probability density function is again generated by the kernel density estimation. This example used data from neuron 380 with sucrose as tastant and 22 trials.

Time 0 is defined as the time of the first lick for which water is present in the spout. Only data after this time point are used in the classification analysis.

The time between two licks, or *lick interval*, is a natural frame of reference to determine the spiking phase. To help in this, we normalize the lick intervals so that all have a *normalized time duration* of 200 time units. Lick intervals that are longer than 200 ms are contracted and those shorter than 200 ms are stretched. This normalization of the lick interval, or time warping, is done uniformly so that the number of spikes per lick interval is not changed and the relative timing of the spikes within a lick interval is maintained. This is illustrated in Fig. 2A,B. The *phase* of the first spike is $\approx 40/200$, or 0.2. The phase of the last spike is $\approx 170/200$, or 0.85. In our analysis, we examine the first 5 lick intervals starting at time 0. Therefore, each spike train vector used

in the analysis contains 1000 elements: 200 for the time points within each of 5 normalized lick intervals. We refer to each such vector as a *processed spike train vector*.

Creating Empirical Rate and Phase Distributions

From the processed spike train vectors, we construct approximate phase and rate probability distributions for each neuron that responds to each stimulus. A phase distribution describes the timing of spikes relative to licks in the processed spike train. To construct this, we first form the union as a multiset of the processed spike trains for that neuron/stimulus pair to create one 1000-dimensional vector for each pair. We convert this distribution, defined only at discrete time points, to a continuous distribution. We then remove the rate information by normalizing the distribution to sum to 1, regardless of the number of spikes considered. To construct a rate distribution, we form a histogram (with bin size of 1) of the number of spikes produced per trial.

Transformation to a continuous distribution is done using a Gaussian Kernel Density Estimator (Pedregosa et al., 2011) as follows. The continuous function that interpolates our recordings for a particular neuron/stimuli pair is

$$\mu(x) = \frac{1}{K} \sum_{i=1}^{K} \frac{1}{\sqrt{2\pi h^2}} \exp\left(-\frac{(x - x_i)^2}{2h^2}\right)$$

where $x \in [0, 999]$, and $(x_1, x_2, \ldots, x_K)$ are the K data points. For phase distributions, the data are the union of all spike times. For rate distributions, the data are the values of the spike frequency histogram. The parameter h is called the bandwidth and is akin to a smoothing parameter - the larger the bandwidth, the greater the smoothing. We use $h = 5$ when calculating Phase PDFs and $h = 2$ when calculating Rate PDFs, using a finer bandwidth when smoothing histograms with a small bin size and a larger bandwith when trying to get a sense of the density of spiking for phase distributions. We verified that the results were stable under a range of bandwidth values for phase functions, so we chose a value on the lower end of the stable range to retain as much variability within the data as possible while maintaining similar results. Similarly, when searching for optimal bandwidth values to use for rate functions, we found that the results are optimal with lower bandwidth, achieving the best classification scores overall with h=2.

This process is illustrated in Fig. 2C, D. Panel C shows the timing of spikes over all 5 lick intervals (black bars). These data are used to construct a probability density function (blue curve) using kernel density estimation. Probability values are low because the time spans all five lick intervals, and the number of data points (spikes), K, is large over that long time span. Panel D illustrates the construction of the spike-rate density function. The process begins with a histogram of the number of spikes per trial for a particular neuron/stimulus pair. These data are then used in the kernel density estimator to generate a smooth, continuous probability density function (blue curve). In this case, the number of data points, K, is the number of different values of spikes per trial that occur in the trials examined.

Bayesian Classifier Design

We quantify the degree to which a neuron successfully distinguishes one stimulus from the others through classification scores. We employ a Bayesian classification scheme that makes use of one or both of the probability density functions described above. The data sets (processed spike trains) were first divided into training (80%) and testing (20%) sets. The spike trains in the training set were used to construct empirical rate and phase distributions as described above. The spike trains in the test set were used to determine the classification score, as described below.

For classification based on phase distributions, each processed spike train with N spikes in the test set is interpreted as N i.i.d. samples $(x_1, \ldots, x_N)$ from a phase distribution for one of the stimuli M stimuli: μ_i^P, $i = 1 \ldots M$. To determine the most likely stimulus (a taste or temperature) $\mathcal{T}_i$, we maximize $P\big(\mathcal{T}_i|(x_1, \ldots, x_N)\big)$ for $i = 1, \ldots, M$. Employing Bayes' theorem, we obtain

$$P\big(\mathcal{T}_i|(x_1, \ldots, x_N)\big) = \frac{P\big((x_1, \ldots, x_N)|\mathcal{T}_i\big)P\big(\mathcal{T}_i\big)}{\sum_{j=1}^{M} P\big((x_1, \ldots, x_N)|\mathcal{T}_j\big)P\big(\mathcal{T}_j\big)} \quad , \tag{1}$$

where $P\big(\mathcal{T}_j\big)$ are the prior probabilities that the observation is from stimulus $\mathcal{T}_j$. To ensure that all stimuli are equally probable, we include an equal number of trials per stimulus (Q) in the analysis, where Q is the smallest number of trials recorded for any stimulus in a given data set. For stimuli for which more than Q trials were performed, excesses were not included in the analysis. Hence, since all stimuli are equally probable, $P\big(\mathcal{T}_j\big) = \frac{1}{M}$. Under the i.i.d. assumption,

Eq. (1) simplifies to

$$P\big(\mathcal{T}_i|(x_1,\ldots,x_N)\big) = L_i^P \Big/ \sum_{j=1}^{M} L_j^P \quad ,$$

where L_j^P is the likelihood,

$$L_j^P = \mu_j^P(x_1)\ldots\mu_j^P(x_N) \quad .$$

A similar process is used in the case in which rate distributions alone are used in the classification. In this case, each processed spike train is interpreted as a single sample y from a rate distribution for one of the stimuli, μ_i^R, $i = 1\ldots M$. To determine the most likely stimulus $\mathcal{T}_i$, we maximize $P\big(\mathcal{T}_i|y\big)$ for $i = 1,\ldots,M$, and from Bayes' theorem,

$$P\big(\mathcal{T}_i|y\big) = \frac{P\big(y|\mathcal{T}_i\big)P\big(\mathcal{T}_i\big)}{\sum_{j=1}^{M} P\big(y|\mathcal{T}_j\big)P\big(\mathcal{T}_j\big)},$$

or with the i.i.d. assumption,

$$P\big(\mathcal{T}_i|y\big) = L_i^R \Big/ \sum_{j=1}^{M} L_j^R,$$

where L_j^R is the likelihood,

$$L_j^R = \mu_j^R(y) \quad .$$

Finally, in the case in which both rate and phase are used in the classification, we maximize the weighted sum of the two probabilities:

$$RP_i = \alpha P\big(\mathcal{T}_i|y\big) + (1-\alpha)P\big(\mathcal{T}_i|(x_1,\ldots,x_N)\big) \tag{2}$$

with weight $\alpha \in [0,1]$. When $\alpha = 0$ only the phase information is used and when $\alpha = 1$ only the rate information is used. The values of α between 0 and 1 use a combination of the two, and are equally weighted when $\alpha = 0.5$.

Using this approach, we obtain a value RP_i for each of the stimuli, and the stimulus with the highest value is selected as the one most likely to produce the spike train. This is done for all elements of the test set, and the *classification score* is the fraction of times the classification is correct. This process is repeated 15 times for each neuron, each with a different partition of spike trains into

training and testing sets. The classification scores are then averaged over these 15 splits to obtain an overall classification score for the neuron.

Support Vector Machine Classification

To validate our Bayesian analysis classification results, we compare them with a similar classification experiment carried out with a Support Vector Machine (SVM), a tool of classical machine learning (Fan et al., 2008; Pedregosa et al., 2011). Roughly, the SVM determines the optimal hyperplanes that separate the data into a specified number of classes. Each of these is associated with a stimulus, based on the labels of the data used to train the SVM. To perform this experiment, the processed spike train vectors for every neuron/stimulus pair were smoothed by convolving the sequence of values 0 and 1 with a Gaussian kernel (a smoothing window of 100 was used). As in Bayesian classification, the processed spike train data were divided into a training set (80%) and a test set (20%). The training set was used to fit the parameters of the SVM model. Using the trained model, each element of the test set was classified. The fraction of correct classifications is then the classification score. This sequence was repeated 15 times for each neuron, with the same random partitions for training and testing sets that were used in Bayesian classification. The average classification score for a single neuron in all 15 iterations is the final classification score for that neuron. See (Neese et al., 2022) for more details on the SVM classifier and smoothing process.

Results

Using a Bayesian classifier to elucidate GC activity

To begin investigating how neurons in the gustatory portion of the insular cortex encode oral information in freely licking mice, we made extracellular recordings using movable bundle tetrodes or silicon probes implanted unilaterally in the GC (Fig. 1). After habituation to head restraint, a group of mildly (1.5 ml per day) water-deprived mice was engaged in a task in which they had to lick a dry spout 6 times to obtain a drop of one of four gustatory stimuli (100 mM sucrose, 50 mM NaCl, 10 mM citric acid, 0.5 mM quinine) and water presented at room temperature. A second group of mice, in a different session, was also trained to receive deionized water at three different non-nociceptive temperatures (14°, 25°

and 36°C). At the end of the training (1 week), the recording session started. In the mice included in the taste dataset, we recorded and analyzed neural activity only in response to gustatory stimuli (Fig. 1B). For the mice included in the temperature dataset, we initially recorded neural activity evoked by taste stimuli presented at room temperature, as explained in (Bouaichi et al., 2023). Following this recording session, we analyze the spiking activity of a single neuron. If taste-selective neurons were detected, the tetrodes or probes were lowered approximately 100 μm and subsequent recording sessions exclusively captured the activity evoked by deionized water at various temperatures. As explained in Bouaichi et al. (Bouaichi et al., 2023), this approach was specifically selected to provide additional functional evidence confirming that neuron responses to thermal stimuli were acquired from the gustatory cortex. In general, for this project, we analyzed taste chemosensory information in 529 GC neurons recorded from 12 wild-type mice, and oral thermal information from 433 GC neurons recorded from 18 wild-type mice (see Methods for additional details).

To begin exploring the neural dynamics of GC neurons with respect to taste chemosensory and thermal information, we used a Bayesian classification approach. For each neuron, the spike trains for a chemosensory or thermosensory experiment were first divided into a training set (80%) and a test set (20%), as described in Methods. Then, the spike trains of the training set were used to construct a spike timing probability distribution function and a spike rate distribution function for each neuron (Fig. 2). These characterize the response properties to the different stimuli for that neuron. For each spike train in the test set, we extracted the phase at which each spike occurred and the spike rate per processed spike train to calculate the probability values. Then, they were added together, weighted by a factor $\alpha \in [0, 1]$ that gives more weight to the phase information if $\alpha < 0.5$ and more weight to the rate information if $\alpha > 0.5$. The result is a number RP_j, which is a measure of how well the spike train matched the characteristic phase and rate distributions of the stimulus j in that neuron (Eq. (2)). The neural response is classified as evoked by stimulus j if the objective function, RP_j, is greater than that of other stimuli. That is, if $RP_j > RP_i$ for all $i \neq j$ and $i = 1, \ldots, M$, where M is the number of different stimuli. The fraction of times that the classification of elements in the test set is correct provides the *classification score* for that neuron.

We know from previous work that the Support Vector Machine (SVM) is an effective tool to correctly classify the spiking responses of neurons to a variety of taste stimuli (Neese et al., 2022). However, the SVM approach has the dis-

advantage of providing very limited information on which aspects of the spike trains made the classification successful. The Bayesian classification scheme has the advantage of providing empirical distributions for the spiking phases and rates for the stimulus/neuron pair and of assigning different weights to their contributions in the classification procedure.

Before continuing with the Bayesian classification approach, we verified that it gives comparable results to the established SVM method in correctly classifying neuronal response to stimuli. Figure 3 compares the Bayesian classification classification scores with those of the SVM classification on the same data sets. For each neuron, the training sets used to form the empirical rate and phase distributions for the Bayesian analysis were also used to determine the SVM parameters. The test sets were used to calculate the classification scores. In panel A, spike trains in response to the four tastants were analyzed, so with random guessing the classification score would be 0.25 with either method. Classification scores exhibit a high degree of comparability, with a consistent spread observed between both methods. (For the Bayesian classification, "optimal" values of $\alpha = 0.875$ and 0.750 were used in panels A and B, the choice of which is described in the next section.) Both methods show that most neurons have scores near 0.25, indicating that most spike trains do not discriminate between tastants. There is also a smaller subset of neurons that have classification rates much higher than random guessing. Because the classification scores for the two methods are close to the diagonal line, the scores for the two methods are similar. Analogous results hold for thermal stimuli (Fig. 3B), again demonstrating that the two classification methods produce similar classification scores. All remaining analyses used the Bayesian classification approach.

Classification using rate and phase is better than either alone

We initially used the Bayesian classifier to compute the classification scores of the gustatory information using the taste dataset. These scores were calculated with different values of α ranging from 0 to 1 in increments of 0.125. The mean classification score ranged from 0.27 to 0.28, slightly exceeding the expected value of 0.25 for random guessing (data not shown). These low values indicate that only a relatively small fraction of GC neurons encode gustatory information, in line with previous studies. Consequently, we narrowed our focus to neurons with classification scores in the top 20%. Averaging over this subset of

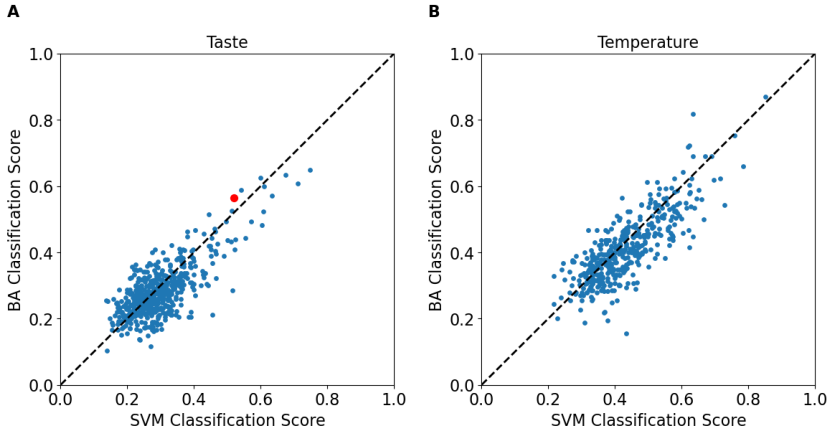

Figure 3: Comparison of classification scores computed with Bayesian and SVM methods. **(A)** The population of 529 neurons in response to 4 tastants (citric acid, NaCl, quinine, and sucrose). The score for random guessing is 0.25. The red point indicates the neuron used in Fig. 2. Points on the dashed line have the same classification score when computed with either method. **(B)** A different population of 433 neurons in response to water at three different temperatures (14°, 25°, and 36°C). The score for random guessing is 0.33. Bayesian analysis scores were computed with $\alpha = 0.875$ and $\alpha = 0.750$, respectively.

neurons, the mean classification scores ranged from 0.37 to 0.40, significantly exceeding the expected score for random guessing (Fig. 4A). In particular, the mean score associated with classification based solely on phase ($\alpha = 0$) was the lowest among all α values. Although the mean score associated with the classification based solely on rate ($\alpha = 1$) was higher, it did not reach the maximum value obtained when combining rate and phase in the classification ($\alpha = 0.875$). These results confirm that the timing of spikes is an important factor in taste decoding (Neese et al., 2022), and that gustatory information is higher when the spike rate change is considered in conjunction with temporal dynamics (Katz et al., 2001). For these reasons, we used this optimal α value in all subsequent analyses of taste classification, unless otherwise noted.

Next, we sought to determine the amount of oral thermal information contained in the GC spike activity. To this end, we used the Bayesian classifier to calculate classification scores of fluid temperature information using our temperature dataset. For a population of 433 neurons, the mean classification scores ranged from 0.38 to 0.41, slightly above the score of 0.33 expected for random guessing (data not shown). When considering only neurons with classi-

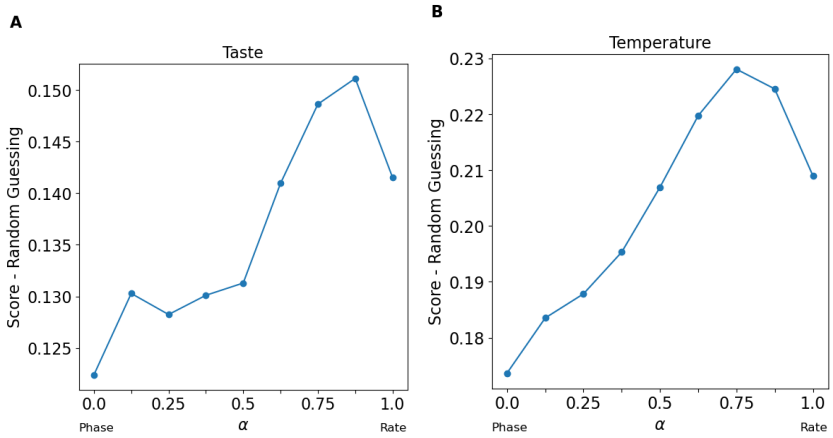

Figure 4: Bayesian-based classification that uses both rate and phase information is optimal. **(A)** Difference between the mean classification scores in animals responding to 4 tastants (citric acid, NaCl, quinine and sucrose) and the random guess score (0.25). For each α, only the top 20% neurons were used in the mean classification score. The optimal α for this subpopulation is $\alpha = 0.875$. **(B)** Difference between mean classification scores in animals responding to water at three different temperatures (14°, 25°, and 36°C) and random guessing (0.33). The analysis performed was similar to that in panel A. The optimal weighting parameter value for the top 20% subpopulation of neurons is $\alpha = 0.750$.

fication scores in the top 20%, the mean classification scores were substantially higher, ranging from 0.18 to 0.23 above the expected score for random guessing (Fig. 4B). Once again, the classification score based on rate alone exceeded that based on phase alone, and the optimal combination of the two included mainly rate, but also phase in the objective function ($\alpha = 0.750$). This optimal value α was used in all subsequent analyses of temperature classification.

Many GC neurons are highly responsive to temperature and taste

Further evaluation of Fig. 4 unveils additional insights. While for classification of either set of stimuli it is best when both phase and rate information are used, it is apparent that the classification scores are higher for thermal stimuli than for taste stimuli. For each value of α, the difference between the classification score and that for random guessing is greater for thermal stimuli compared to gustatory stimuli. To delve deeper into this observation, we constructed

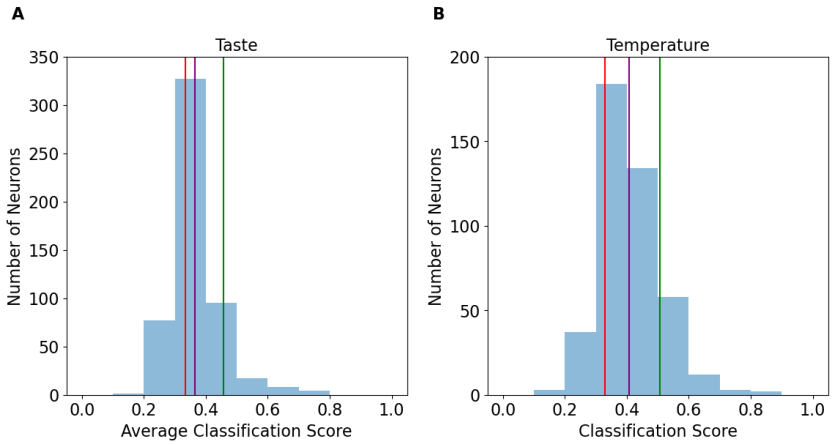

Figure 5: Comparison of three-way classification tasks. **(A)** Histogram of average classification scores using tastant triplets. The mean for all triplets is 0.365, while the mean for each of the four combinations of triplets of tastants is 0.372 (citric acid, NaCl, quinine), 0.364 (citric acid, NaCl, sucrose), 0.359 (citric acid, quinine, sucrose), and 0.364 (NaCl, quinine, sucrose). **(B)** Histogram of classification scores using three water temperatures (14°, 25° and 36°C). In both histograms, the bin size for the classification scores is 0.1. The expected score for random guessing is shown with the red vertical line at 0.33. The mean of the distribution is shown as a violet line. The mean plus one standard deviation is shown as a green line.

histograms of the Bayesian classification scores. For a fair comparison between the four tastants examined and the three temperatures, the tastant histogram was constructed using triplets of tastants. In other words, each classification score for a tastant corresponds to the task of discriminating between three tastants. There are four such tastant triplets, and the classification score for each neuron was determined as the average of its scores computed for each triplet. These averages were used to construct the histogram.

In Fig. 5A, the histogram displays a peak at 0.3, aligned with the value 0.33 for random guessing. The mean score for tastant triplets in this distribution is 0.365, surpassing the expected random guess score. Additionally, 10% of the neurons exhibit high classification scores, with an average above the mean plus one standard deviation. In contrast, Fig. 5B presents a histogram for discriminating between three water temperatures, showing a more rightward skew. Although the peak remains at 0.3, indicative of random guessing, a substantial portion of neurons achieve higher scores. The mean classification score in this histogram reaches 0.399, surpassing that of the tastant triplets. Furthermore, 15% of neurons exceed the mean plus one standard deviation.

Next, we investigate whether all chemosensory and thermal stimuli are equally decoded or whether the GC spike activity included in our two datasets enables some tastes or temperatures to be discriminated more easily than others. To address this point, we specifically selected neurons with classification scores in the top 20% for taste or temperature classification. Figure 6 shows the results of this analysis. The color coding in each bar illustrates how a spike train produced by a neuron was classified. The labels on the x-axis indicate the actual stimulus for the spike train. In panel A, for instance, more spike trains associated with the citric acid stimulus were classified as citric acid (blue region at the bottom of the first bar) than as any other stimulus. When a spike train was misclassified, the fraction of misclassifications was similar across the three other tastant labels. Similar trends were observed for spike trains in response to NaCl and quinine. Sucrose generated the smallest fraction of correct classifications; the fraction of spike trains incorrectly classified as citric acid was comparable to the fraction correctly classified as sucrose. These data suggest that the top performing GC neurons examined were more capable of discriminating citric acid, NaCl, and quinine than sucrose. A similar analysis was conducted for the temperature dataset (Fig. 6B). Spike trains generated in response to cool water (14°C) were correctly classified almost 60% of the time (first bar). The most common misclassification of cool water was water at room temperature

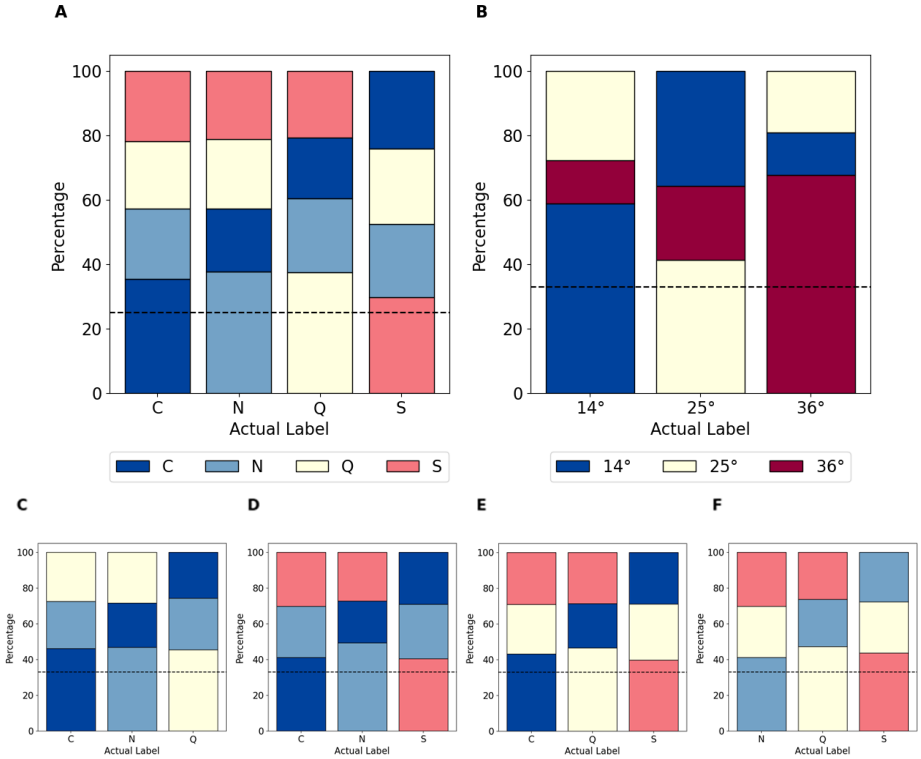

Figure 6: Percentage of correct and incorrect classifications. **(A)** Spike train classification from the neurons that performed at the top 20% for taste. The color corresponds to the way the spike train was classified. The label on the x-axis is the actual stimulus for the spike train. C=citric acid, N=NaCl, Q=quinine, and S=sucrose. The correct classifications are at the bottom of each bar. The black horizontal dashed line is the expected score for random guessing. **(B)** Spike train classification from the neurons that performed at the top 20% for temperature. The fraction of correct classifications was much higher for cold and warm temperatures than for room temperature. **(C–F)** Spike train classification for tastant triplets.

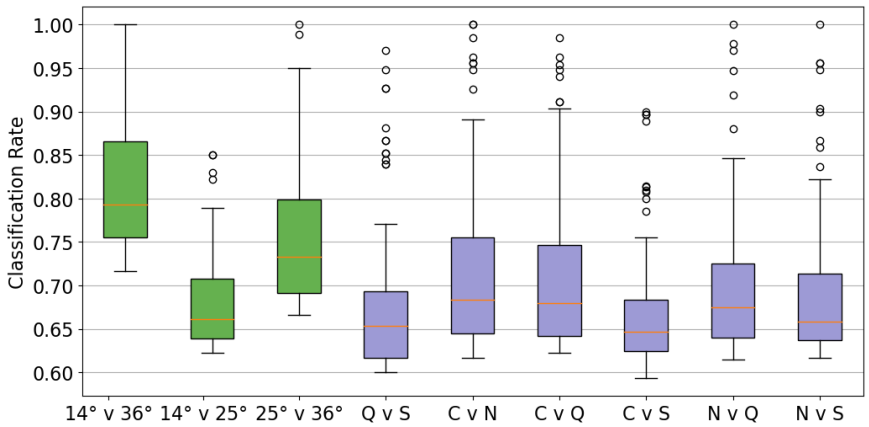

Figure 7: Comparison of classification scores for pairs of temperatures and tastes, using neurons scoring in the top 20%. Temperature scores are in green, taste scores in violet. C=citric acid, N=NaCl, Q=quinine, and S=sucrose. The orange line in each box indicates the median score, and outliers are represented by open circles.

(25°C, yellow region of the first bar). Water at room temperature produced the smallest percentage of correct classifications (second bar), with most misclassifications being the cool temperature. Water at a warm temperature (36°C) produced the highest percentage of correct classifications (third bar), with the most common misclassification also being room temperature.

To more directly compare the classification of responses to taste vs. water temperature, we focus on the tastant triplets in Fig. 6C-F. This analysis shows that the percentage of correct classifications for tastant triplets was always lower than that for warm and cool water (Fig. 6B) and was instead comparable to that for water at room temperature. For the tastant triplets, the highest percentage of correct classifications was for NaCl in the (citric acid, NaCl, and sucrose) triplet. Here, there were 49% correct classifications, far below 61% for cool water and 66% for warm water.

This is further confirmed by studying the classification of stimuli in pairs, shown in Fig. 7. Here, we compare the distribution of classification scores for pairs of stimuli using neurons in the top 20% of each dataset (86 neurons for the Temperature dataset and 105 neurons for the Taste dataset). Visual inspection of the box plots indicates that the median classification scores obtained for thermal stimuli at 14°C and 36°C, the two thermal stimuli with the highest temperature contrast, are above any other, just below 80%. We performed a

	14°C v 36°C	14°C v 25°C	25°C v 36°C	Q v S	C v N	C v Q	C v S	N v Q
14°C v 25°C	$< 2^{-16}$	-	-	-	-	-	-	
25°C v 36 °C	5.30^{-05}	4.60^{-07}	-	-	-	-	-	-
Q v S	$< 2^{-16}$	1	3.20^{-08}	-	-	-	-	-
C v N	2.30^{-13}	0.05661	0.16047	0.016	-	-	-	-
C v Q	2.10^{-13}	0.05903	0.15441	0.01679	1	-	-	-
C v S	$< 2^{-16}$	1	2.90^{-11}	1	0.00014	0.00014	-	-
N v Q	$< 2^{-16}$	1	0.0003	1	1	1	0.12378	-
N v S	$< 2^{-16}$	1	3.30^{-05}	1	0.99108	1	0.52713	1

Table 1: This table presents the p values of pairwise comparisons between oral stimuli using the Bonferroni correction method to adjust for multiple testing (type I error) associated with figure 7. Significant p values ($p < 0.05$) are indicated in red.

one-way analysis of variance (ANOVA) to determine if there were significant differences in classification scores between the different pairs. The ANOVA resulted in a statistically significant result ($F(8, 879) = 28.03$, $p < 0.001$), indicating that the classification scores are not equal in the stimulus pair tested. To further examine the differences between pairs, we performed post hoc pairwise comparisons using the Bonferroni correction method to adjust for multiple tests (Table 1). Our results show that discrimination using GC neuron spike trains is more successful with warm versus cool water stimuli - particularly those with the strongest contrast (i.e., 14° vs. 36°C) than with any two tastants at room temperature.

Stimulus identification over individual lick intervals

Our next objective is to dive deeper into the temporal dynamics of chemosensory and thermal information processing in GC neurons. Thus far, our analysis has focused primarily on spike trains that span five consecutive lick intervals, and the first lick occurs when the stimulus is delivered. However, an intriguing question arises: how robustly are the chemo- and thermosensory stimuli encoded within spike trains over post-stimulus lick intervals compared to the entire five-lick duration? We also wish to explore whether classification performance varies significantly between individual lick intervals, potentially shedding light on similarities or differences in the temporal dynamics of encoding taste and temperature within the gustatory cortex. To address these questions, we performed a Bayesian classification analysis using portions of processed spike trains that occurred during individual lick intervals (see Figure 8). This analysis used spike trains for neurons that scored the highest 20% for taste or temperature when considering the duration of five licks. Figures 8A and B depict

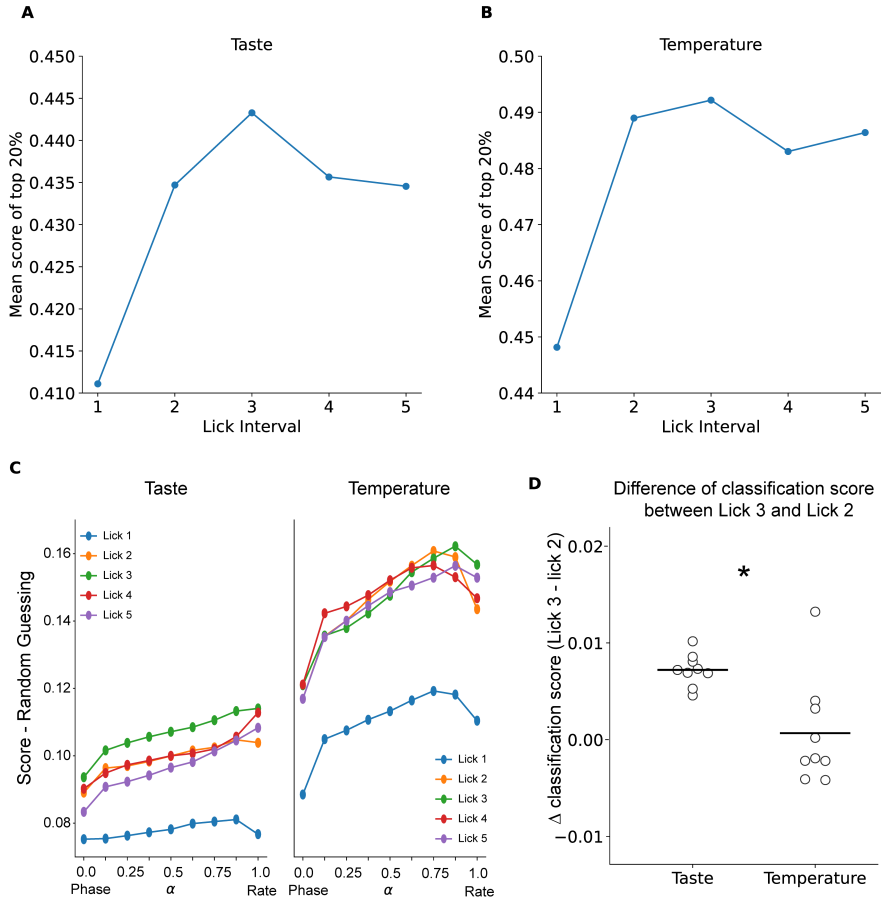

Figure 8: Classification scores based on individual lick intervals. **(A)** Calculated as the average of scores for taste triplets. **(B)** Based on three different water temperatures. Each point represents the mean classification score from the top 20% of neurons when considering classification scores over that particular lick interval only. **(C)** Left panel shows the difference between mean classification score and random guessing for the average of all taste triplets over the 5 different lick intervals across the range of α values. The data set from panel A is used in the analysis. The right panel shows a similar analysis, but for the three water temperatures. The data set from panel B is used. **(D)** Difference in classification scores between lick interval 3 and lick interval 2, for taste and thermal stimuli. Each point represents the score difference for a particular value of α. The horizontal bars are the average values. *p<0.05.

the mean classification score in the different lick intervals for the taste triplets and the temperature, respectively. Visual inspection of the graphs reveals two main points. First, the initial lick interval, which corresponds to the time period approximately 125 ms after stimulus delivery, contains both chemosensory and thermal information. Second, while temperature classification reaches a plateau during the second lick interval, taste classification appears to take longer to reach its peak score, which occurs in the third lick interval. To further investigate this trend, we calculated classification scores for different lick intervals and different rate/phase weighting values α (Fig. 8C). For both taste and temperature, although the optimal α varies somewhat from lick interval to lick interval, the performance is best for values of α close to, but less than, 1 (Fig. 8C). This indicates that classification weighted heavily, but not entirely, to the spike rate is optimal. Furthermore, while the classification scores for temperature beyond the first lick interval are comparable between the α values, for taste stimuli the classification score is highest during the third lick interval regardless of α (Fig. 8C). Analysis of differences in all classification scores using the second and third lick intervals revealed early success in classification of thermal stimuli compared to taste stimuli (Fig. 8D; ttest: $t(9.4)=3.39$, $p=0.0073$). This suggests a potentially differential processing of thermal and chemosensory stimuli within the GC, confirming that the timing of neural events can contribute to the representation of oral stimuli (Lemon and Katz, 2007) and that somatosensory input can be encoded earlier than chemosensory input (Katz et al., 2001).

Discussion

Experimental evidence from electrophysiological and optical imaging studies shows that neurons in the gustatory cortex represent non-gustatory multimodal stimuli experienced before and/or during sampling (Chen et al., 2021; Vincis and Fontanini, 2016; Samuelsen and Fontanini, 2017; Maier, 2017; Livneh et al., 2017; Gardner and Fontanini, 2014; Samuelsen et al., 2012). Of particular relevance here are studies that have examined how neurons in the GC respond to other intraoral somatosensory characteristics, such as variations in temperature. Pioneering work in anesthetized rats (Yamamoto et al., 1981; Kosar et al., 1986) and work in the primate insular/opercular cortex (Verhagen et al., 2004; Kadohisa et al., 2005) indicates that thermal changes in fluid solutions appear to modulate the activity of a subset of GC neurons. Furthermore, our recent

work has shown that GC neurons were capable of reliably responding to and discriminating a wide range of innocuous oral temperatures of deionized water in a mostly monotonic manner (Bouaichi et al., 2023). Although these observations underscore the crucial role of the GC in the integration of gustatory and thermal signals, they leave unresolved the issue of whether and which of these oral sensory modalities is more dominantly represented in the GC.

Given the role of the GC in processing taste stimuli (Mukherjee et al., 2019; Chen et al., 2021; Fletcher et al., 2017; Katz et al., 2001), one could speculate that taste-related sensory input could inherently have a more prominent representation within this cortical region. This would align with intuitive - but admittedly overly simplistic - expectations, considering the taste cortex function in gustation. However, increasing evidence of nuanced and multifaceted involvement of the GC in the processing of not only gustatory, but also other components of oral stimuli relevant to flavor (Rudenga et al., 2010; Samuelsen and Fontanini, 2017; Verhagen et al., 2004; De Araujo et al., 2003; Vincis and Fontanini, 2016; Bouaichi et al., 2023; De Araujo and Simon, 2009; Maier, 2017) introduces the intriguing possibility that temperature information might play a more significant or equally vital role in its sensory integration processes.

In our study, we collected recordings of spiking activity from more than 900 individual GC neurons in mice allowed to freely lick to receive a small drop (3 μl) of one of four liquid gustatory stimuli (sucrose, NaCl, citric acid and quinine) at room temperature, or deionized water at one of three different non-nociceptive temperatures (14°, 25° and 36°C). We then used a Bayesian analysis approach to compute classification scores for spike trains, taking into account both the rate and phase (the timing of spikes within the lick cycle) codes in response to the different oral stimuli. Our analysis revealed that fluid temperature exerts a more robust neural encoding, making it more neurally salient compared to taste information. Using the best-performing neurons for encoding (top 20% for chemosensory and thermal information), our comparisons of classification scores between different stimuli revealed that neuronal responses in the GC distinguish more effectively between deionized water at warm and cool temperatures, particularly at the extremes of our temperature range (e.g., 14°C vs. 36°C), than between any pair of chemosensory stimuli presented at room temperature. Although several recent works have shown how taste responses in the GC are not spatially distributed, but rather scattered without a clear topographic organization (Chen et al., 2021; Fletcher et al., 2017; Levitan et al., 2019), it could be hypothesized that our recordings were predominantly

from regions of the GC that are not highly sensitive to taste (see, for example, Chen et al. (2011)). However, this possibility is countered by the nature of our experimental approach, as our data set (see Bouaichi and Vincis (2020); Neese et al. (2022); Bouaichi et al. (2023)) includes recordings from a broad section of the anteroposterior axis of the GC.

Our analysis also reveals that the encoding of sensory information by neurons in the gustatory cortex evolves across licks post-stimulus and involves both the rate and phase of spiking, although the spike rate plays a more dominant role. Another observation is that the temporal dynamics of signal encoding in the GC for the two modalities differs, with thermal stimuli reaching peak decoding earlier than taste stimuli (Fig. 8). This result underscores a potential fundamental difference in the way GC processes these two types of oral signals. This finding is closely aligned with previous research in rats, which used intraoral cannulae (IOCs) to deliver taste stimuli, providing insight into the temporal dynamics of cortical taste processing (Katz et al., 2001). In this seminal study by Katz and colleagues, analysis of the time courses of GC neural responses to taste revealed that modulation of the GC firing rate arose from separable processes, each corresponding to distinct temporal epochs, with the first two representing an early somatosensory input (i.e., the "touch" evoked by squirting the taste solution in the mouth) followed by a later chemosensory input (represented by taste identity).

The questions that then arise are: 1) what functional role could thermal oral signals, encoded by GC neurons, play in the context of sensory processing and behavioral responses? and 2) why does the GC (as opposed to other relevant cortical areas such as the oral somatosensory cortex) appear to be an important cortical site for the encoding of thermal oral signals? For the first question, we can safely speculate that these oral signals are integral to flavor processing and behavioral responses, particularly in relation to consummatory behavior. The gustatory cortex has been implicated in functions related to taste processing (Katz et al., 2001; Blonde et al., 2015; Sadacca et al., 2012), taste learning (Schier et al., 2016; Kayyal et al., 2021; Yiannakas et al., 2021; Arieli et al., 2022) and expectation (Samuelsen et al., 2012; Gardner and Fontanini, 2014; Vincis and Fontanini, 2016; Livneh et al., 2017), but also in taste-based decision making (Mukherjee et al., 2019; Vincis et al., 2020), highlighting its role not only in sensory processing, but also in modulating consummatory behaviors. Therefore, encoding oral thermal signals by the GC could help improve the fidelity of food evaluation processes, integrating temperature as a crucial parameter in

evaluating food quality and palatability (Zellner et al., 1988; Moskowitz, 1973; Torregrossa et al., 2012). Furthermore, the difference in the temporal dynamics of the encoding of the two modalities underlies a hierarchical processing model that fits well with the ecological necessity of a rapid assessment of potential food items based on their thermal attributes, which could have direct implications for survival, especially in environments where temperature can signal freshness or potential hazard of consumed substances.

Regarding the second question, previous experimental evidence may provide information. A study in humans (Craig et al., 2000) and a more recent study in rodents (Vestergaard et al., 2023) indicated that the posterior insular cortex, a region located closely but posterior to the areas targeted in our recordings, functionally represents and underlies the thermosensory perception of the skin. This, together with our findings, points to the possibility of a postero-anterior gradient across the insular cortex for representing thermal information, extending from extraoral to oral thermal signals. This gradient could imply that the gustatory cortex, located within this continuum, is optimally positioned to integrate oral thermal information as a component of its broader role in sensory processing. This specialization might reflect an evolutionary adaptation, prioritizing the gustatory cortex for oral thermal sensing due to its direct implications for feeding and the evaluation of food stimuli, in contrast to the more general body temperature regulation functions possibly attributed to more posterior regions of the insular cortex.

In general, our results further confirm that neurons in the gustatory cortex not only process taste information, but are also capable of integrating thermal signals from the oral cavity. This dual capacity underscores the importance of considering temperature as a critical dimension in future studies of cortical taste coding. Temperature modulation may significantly affect the encoding of taste information, potentially altering our understanding of how GC contributes to nuanced perception of flavor. Our evidence suggesting that thermal stimuli evoke a more pronounced neural response than taste stimuli invites further investigation of the mechanisms underlying this phenomenon and the role of the GC in processing taste information as a function of stimulus temperature.

Acknowledgements

This research was supported by grant number DMS 2324962 from the National Science Foundation to TN, MB, RV, and RB, and by grant number R01 DC-

019326 from the National Institute on Deafness and Other Communication Disorders to RV.

References

Arieli E, Younis N, Moran A (2022) Distinct progressions of neuronal activity changes underlie the formation and consolidation of a gustatory associative memory. *Journal of Neuroscience* 42:909–921.

Blonde GD, Bales MB, Spector AC (2015) Extensive lesions in rat insular cortex significantly disrupt taste sensitivity to NaCl and KCl and slow salt discrimination learning. *PLoS One* 10:e0117515.

Bouaichi CG, Odegaard KE, Neese C, Vincis R (2023) Oral thermal processing in the gustatory cortex of awake mice. *Chemical Senses* p. bjad042.

Bouaichi CG, Vincis R (2020) Cortical processing of chemosensory and hedonic features of taste in active licking mice. *Journal of Neurophysiology* 123:1995–2009.

Buccino AP, Hurwitz CL, Garcia S, Magland J, Siegle JH, Hurwitz R, Hennig MH (2020) Spikeinterface, a unified framework for spike sorting. *Elife* 9:e61834.

Cerf-Ducastel B, Van de Moortele PF, MacLeod P, Le Bihan D, Faurion A (2001) Interaction of gustatory and lingual somatosensory perceptions at the cortical level in the human: a functional magnetic resonance imaging study. *Chemical Senses* 26:371–383.

Chen K, Kogan JF, Fontanini A (2021) Spatially distributed representation of taste quality in the gustatory insular cortex of behaving mice. *Current Biology* 31:247–256.

Chen X, Gabitto M, Peng Y, Ryba NJ, Zuker CS (2011) A gustotopic map of taste qualities in the mammalian brain. *Science* 333:1262–1266.

Craig AD, Chen K, Bandy D, Reiman EM (2000) Thermosensory activation of insular cortex. *Nature Neuroscience* 3:184–190.

De Araujo IE, Simon SA (2009) The gustatory cortex and multisensory integration. *International Journal of Obesity* 33:S34–S43.

De Araujo IE, Kringelbach ML, Rolls ET, McGlone F (2003) Human cortical responses to water in the mouth, and the effects of thirst. *Journal of Neurophysiology* 90:1865–1876.

Dikecligil GN, Graham DM, Park IM, Fontanini A (2020) Layer-and cell type-specific response properties of gustatory cortex neurons in awake mice. *Journal of Neuroscience* 40:9676–9691.

Fan RE, Chang KW, Hsieh CJ, Wang XR, Lin CJ (2008) Liblinear: A library for large linear classification. *J. Mach. Learn. Res.* 9:1871–1874.

Fletcher ML, Ogg MC, Lu L, Ogg RJ, Boughter JD (2017) Overlapping representation of primary tastes in a defined region of the gustatory cortex. *Journal of Neuroscience* 37:7595–7605.

Gardner MP, Fontanini A (2014) Encoding and tracking of outcome-specific expectancy in the gustatory cortex of alert rats. *Journal of Neuroscience* 34:13000–13017.

Jezzini A, Mazzucato L, La Camera G, Fontanini A (2013) Processing of hedonic and chemosensory features of taste in medial prefrontal and insular networks. *Journal of Neuroscience* 33:18966–18978.

Kadohisa M, Rolls ET, Verhagen JV (2005) Neuronal representations of stimuli in the mouth: the primate insular taste cortex, orbitofrontal cortex and amygdala. *Chemical Senses* 30:401–419.

Katz DB, Simon S, Nicolelis MA (2001) Dynamic and multimodal responses of gustatory cortical neurons in awake rats. *Journal of Neuroscience* 21:4478–4489.

Kayyal H, Chandran SK, Yiannakas A, Gould N, Khamaisy M, Rosenblum K (2021) Insula to mPFC reciprocal connectivity differentially underlies novel taste neophobic response and learning in mice. *Elife* 10:e66686.

Kosar E, Grill HJ, Norgren R (1986) Gustatory cortex in the rat. i. physiological properties and cytoarchitecture. *Brain Research* 379:329–341.

Lemon CH (2021) Tasting temperature: neural and behavioral responses to thermal stimulation of oral mucosa. *Current Opinion in Physiology* 20:16–22.

Lemon CH, Katz DB (2007) The neural processing of taste. *BMC neuroscience* 8:1–8.

Levitan D, Lin JY, Wachutka J, Mukherjee N, Nelson SB, Katz DB (2019) Single and population coding of taste in the gustatory cortex of awake mice. *Journal of Neurophysiology* 122:1342–1356.

Livneh Y, Ramesh RN, Burgess CR, Levandowski KM, Madara JC, Fenselau H, Goldey GJ, Diaz VE, Jikomes N, Resch JM et al. (2017) Homeostatic circuits selectively gate food cue responses in insular cortex. *Nature* 546:611–616.

Maier JX (2017) Single-neuron responses to intraoral delivery of odor solutions in primary olfactory and gustatory cortex. *Journal of Neurophysiology* 117:1293–1304.

Moskowitz HR (1973) Effects of solution temperature on taste intensity in humans. *Physiology & Behavior* 10:289–292.

Mukherjee N, Wachutka J, Katz DB (2019) Impact of precisely-timed inhibition of gustatory cortex on taste behavior depends on single-trial ensemble dynamics. *Elife* 8:e45968.

Neese C, Bouaichi CG, Needham T, Bauer M, Bertram R, Vincis R (2022) Active licking shapes cortical taste coding. *Journal of Neuroscience* 42:8658–8669.

Pachitariu M, Steinmetz NA, Kadir SN, Carandini M, Harris KD (2016) Fast and accurate spike sorting of high-channel count probes with kilosort. *Advances in Neural Information Processing Systems* 29.

Pedregosa F, Varoquaux G, Gramfort A, Michel V, Thirion B, Grisel O, Blondel M, Prettenhofer P, Weiss R, Dubourg V, Vanderplas J, Passos A, Cournapeau D, Brucher M, Perrot M, Duchesnay E (2011) Scikit-learn: Machine learning in Python. *Journal of Machine Learning Research* 12:2825–2830.

Rudenga K, Green B, Nachtigal D, Small D (2010) Evidence for an integrated oral sensory module in the human anterior ventral insula. *Chemical Senses* 35:693–703.

Sadacca BF, Rothwax JT, Katz DB (2012) Sodium concentration coding gives way to evaluative coding in cortex and amygdala. *Journal of Neuroscience* 32:9999–10011.

Samuelsen CL, Fontanini A (2017) Processing of intraoral olfactory and gustatory signals in the gustatory cortex of awake rats. *Journal of Neuroscience* 37:244–257.

Samuelsen CL, Gardner MP, Fontanini A (2012) Effects of cue-triggered expectation on cortical processing of taste. *Neuron* 74:410–422.

Samuelsen CL, Vincis R (2021) Cortical hub for flavor sensation in rodents. *Frontiers in Systems Neuroscience* 15:772286.

Schier LA, Blonde GD, Spector AC (2016) Bilateral lesions in a specific subregion of posterior insular cortex impair conditioned taste aversion expression in rats. *Journal of Comparative Neurology* 524:54–73.

Small DM (2012) Flavor is in the brain. *Physiology & Behavior* 107:540–552.

Spector AC, Travers SP (2005) The representation of taste quality in the mammalian nervous system. *Behavioral and Cognitive Neuroscience Reviews* 4:143–191.

Spence C (2015) Multisensory flavor perception. *Cell* 161:24–35.

Stapleton JR, Lavine ML, Wolpert RL, Nicolelis MA, Simon SA (2006) Rapid taste responses in the gustatory cortex during licking. *Journal of Neuroscience* 26:4126–4138.

Torregrossa AM, Bales MB, Breza JM, Houpt TA, Smith JC, Contreras RJ (2012) Water restriction and fluid temperature alter preference for water and sucrose solutions. *Chemical Senses* 37:279–292.

Verhagen JV, Kadohisa M, Rolls ET (2004) Primate insular/opercular taste cortex: neuronal representations of the viscosity, fat texture, grittiness, temperature, and taste of foods. *Journal of Neurophysiology* 92:1685–1699.

Vestergaard M, Carta M, Güney G, Poulet J (2023) The cellular coding of temperature in the mammalian cortex. *Nature* 614:725–731.

Vincis R, Chen K, Czarnecki L, Chen J, Fontanini A (2020) Dynamic representation of taste-related decisions in the gustatory insular cortex of mice. *Current Biology* 30:1834–1844.

Vincis R, Fontanini A (2016) Associative learning changes cross-modal representations in the gustatory cortex. *Elife* 5:e16420.

Vincis R, Fontanini A (2019) Central taste anatomy and physiology. *Handbook of Clinical Neurology* 164:187–204.

Yamamoto T, Yuyama N, Kawamura Y (1981) Cortical neurons responding to tactile, thermal and taste stimulations of the rat's tongue. *Brain Research* 221:202–206.

Yiannakas A, Chandran SK, Kayyal H, Gould N, Khamaisy M, Rosenblum K (2021) Parvalbumin interneuron inhibition onto anterior insula neurons projecting to the basolateral amygdala drives aversive taste memory retrieval. *Current Biology* 31:2770–2784.

Zellner DA, Stewart W, Rozin P, Brown J (1988) Effect of temperature and expectations on liking for beverages. *Physiology & Behavior* 44:61–68.